

Using $Z \rightarrow \tau\tau$ events to calculate Tau ID scale factors using high p_T Tau leptons

Diego Baron

Supervisor: Prof. Terence Wyatt

Examiner: Dr. Marco Gersabeck

University of Manchester

Faculty of Science and Engineering

School of Physics and Astronomy

April, 2020

Writing Period

05. 07. 2016 – 05. 10. 2016

Supervisor

Prof. Terence Wyatt

Examiner

Dr. Marco Gersabeck

Declaration

I hereby declare, that I am the sole author and composer of my thesis and that no other sources or learning aids, other than those listed, have been used. Furthermore, I declare that I have acknowledged the work of others by providing detailed references of said work.

I hereby also declare, that my Thesis has not been prepared for another examination or assignment, either wholly or excerpts thereof.

Place, Date

Signature

Abstract

foo bar

Contents

1	Introduction	1
2	Tau physics overview	3
2.1	The Tau Lepton	3
2.2	Lepton Universality	6
3	Analysis	9
3.1	The LHC and the ATLAS experiment	9
3.2	Tau Reconstruction and Identification on the ATLAS detector	9
3.3	Monte Carlo Samples	12
3.4	The Collinear Approximation	12
3.5	Event Selection	12
4	Results	15
4.1	$\mu\tau$ Final state	15
4.2	$e\tau$ Final state	15
4.3	Monte Carlo and data discrepancies	15
5	Conclusions and prospects	17
	Bibliography	21

List of Figures

1	Tau leptonic decay mode. Tau lepton is kinematically allowed to decay into muons or electrons, not that in this decay mode two neutrinos of different flavour are produced.	4
2	Tau hadronic decay mode. Tau lepton is kinematically allowed only to decay into hadrons containing up, down and strange quarks. This results on final states containing multiple pions or kaons [1].	5
3	Combined results from BABAR,Belle and LHCb with $1-\sigma$ contour. The average calculated by the Heavy Flavour Averaging Group [2] is compared with the SM predictions.	8
4	Graphic representation that shows the main differences between a 3-prong τ_{had} and a jet originated from quark or gluon radiation (QCD jets). Charged hadrons are shown as thick lines and dashed lines represent neutral particles. The green cone is drawn to depict how τ_{had} product decays are more collimated.	11
5	Comparisson between the performance of BDT and RNN algorithms. Working points are shown as points. Notice there is a trade off between true τ_{had} efficiency and background rejection power. Taken from [10]	12
6	Distribution of the RNN scores for true and fake τ_{had} candidates for 1-prong (a) and 3-prong (b) cases. Taken from [10].	13
7	Caption that appears in the figlist	18

List of Tables

1	Tau hadronic decay modes branching fractions.	6
2	Working points with their corresponding true τ_{had} selection efficiency and the background rejection factors. The scores are shown for both RNN and BDT algorithms.	12
3	Table caption	17

List of Algorithms

1 Introduction

2 Tau physics overview

This chapter is a review of the Tau lepton properties. They include the nature of this particle, its interactions with other the Standard Model (SM) particles, its main decay modes and the physics implications of the so called Lepton Universality (LU), one of the SM predictions.

2.1 The Tau Lepton

The Tau is a spin- $\frac{1}{2}$, electrically charged particle that belongs to the same family of particles as the electron, the muon and the neutrinos, they are all called *leptons*. Leptons are elementary particles that interact only via the weak and electromagnetic interactions, for the latter case only if they have electric charge.

The first hints for the tau existence came from experiments conducted at the Stanford Linear Accelerator Center and Lawrence Berkeley National Laboratory [3]. They discovered 64 events of the form:

$$e^+ + e^- \rightarrow e^\pm + \mu^\mp + \geq 2 \text{ undetected particles}, \quad (1)$$

for which there was no conventional explanation at the time. Later on, it was discovered that these events came from the production of a pair of new particles,

two taus that subsequently decayed onto one electron, a muon and four neutrinos. Events like,

$$e^+ + e^- \rightarrow \tau^+ \tau^- \rightarrow e^\pm + \mu^\mp + 4\nu, \quad (2)$$

were later explored to derive tau mass and spin, confirming the existence of a third generation of leptons.

The tau mass being 1776.86 ± 0.12 MeV allows this lepton not only to decay into the other lighter lepton generations (*leptonic tau decays*), as its shown on Fig.1 , but into *hadrons*. These are particles made of quarks, all the decay channels of the tau containing hadrons in the final state are called *hadronic tau decays*. An example of this decay mode is shown in Fig.2

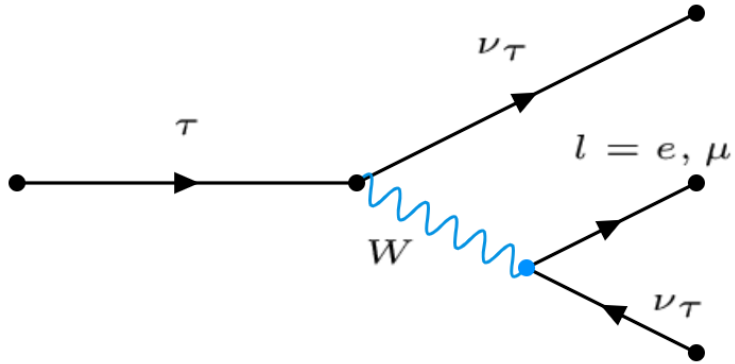


Figure 1: Tau leptonic decay mode. Tau lepton is kinematically allowed to decay into muons or electrons, not that in this decay mode two neutrinos of different flavour are produced.

Naively, if we were to estimate the branching fraction for hadronic and leptonic tau decay modes, defined as:

$$\beta(\tau \rightarrow X \nu_\tau) = \frac{\Gamma(\tau \rightarrow X \nu_\tau)}{\Gamma_{\text{tot}}}, \quad (3)$$

where X could be any group of leptons or hadrons and Γ_{tot} is the total decay width for the tau, we could argue that the contribution from the hadronic decays triples the contribution for one of the leptonic modes. This is because in any hadronic decay,

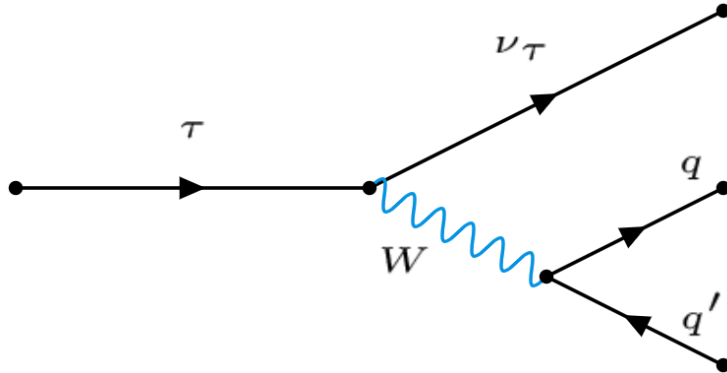


Figure 2: Tau hadronic decay mode. Tau lepton is kinematically allowed only to decay into hadrons containing up, down and strange quarks. This results on final states containing multiple pions or kaons [1].

we would have to count 3 different diagrams, like the one in Fig.2 because of the 3 colour possibility for the quarks.

Thus,

$$\beta(\tau \rightarrow l\nu_l\nu_\tau) \approx 20\% \quad l = e, \mu; \quad (4)$$

$$\beta(\tau \rightarrow X\nu_\tau) \approx 60\% \quad X = \text{hadrons+neutrinos}. \quad (5)$$

In fact, this naive estimation is not so bad. Actual values for the leptonic branching ratios are [4]:

$$\beta(\tau \rightarrow e\nu_e\nu_\tau) = 17.82 \pm 0.04\% \quad (6)$$

$$\beta(\tau \rightarrow \mu\nu_\mu\nu_\tau) = 17.39 \pm 0.04\%, \quad (7)$$

and the small difference is due to the mass variation between the muon and the electron.

On the other hand, the hadronic decays of the tau are more varied and can contain much more particles in the final states. The vast majority of hadronic tau decays have charged or neutral pions in the final states, but more exotic decays including

Decay mode	Branching fraction
$\pi^\pm \nu_\tau$	11.1 %
$\pi^\pm \pi^0 \nu_\tau$	25.4%
$\pi^\pm \geq 2\pi^0 \nu_\tau$	9.1%
$3\pi^\pm \nu_\tau$	9.1%
$3\pi^\pm \geq 1\pi^0 \nu_\tau$	4.6%
others	5.5%

Table 1: Tau hadronic decay modes branching fractions.

kaons also happen. Branching ratios for the most important tau hadronic decays are showed in Table 1.

2.2 Lepton Universality

The SM predicts that all charged leptons (e, μ, τ) interact via the electromagnetic and weak forces and explains that this interactions can be seen as the interchange of *vector bosons*, the photon (γ) and the W and Z bosons respectively. Specifically, in the SM the form of the interaction does not depend on the lepton generation. This feature of the SM is called *lepton universality* and it can be understand as that many physical process for electrons, muons and taus are almost identical copies of each other (although some small discrepancies arise from the fact that lepton masses are different and extrictly speaking lepton universality is not a exact symmetry).

For instance, tau leptonic decay widths are an outstanding way to test lepton universality hypothesis. If we start considering muon decay, at low energy we can consider this process to be a point like interaction well described by Fermi theory [5]. In this case, if we approximate the electron and neutrinos as being massless particles, a dimensionally correct expression for the width will be of the form:

$$\Gamma(\mu \rightarrow e + \nu_e + \nu_\mu) = K G_F^2 m_\mu^5, \quad (8)$$

where $G_F = 1.1666 \times 10^{-5}$ GeV $^{-2}$ is the Fermi coupling constant and K is a constant that depends on the form of the interaction. If we assume lepton universality holds, the respective widths for the leptonic tau decay modes, will have the form:

$$\Gamma(\tau \rightarrow e + \nu_e + \nu_\tau) = K G_F^2 m_\tau^5 \quad (9)$$

$$\Gamma(\tau \rightarrow \mu + \nu_\mu + \nu_\tau) = \Gamma(\tau \rightarrow e + \nu_e + \nu_\tau), \quad (10)$$

and this explains why to a good approximation leptonic branching fractions for tau decay are equal. Moreover, we can obtain a relation between tau and muon lifetimes. We know that,

$$\tau_l = \frac{1}{\Gamma_{\text{Tot}}} = \frac{\beta(l \rightarrow e\nu_e\nu_l)}{\Gamma(l \rightarrow e\nu_e\nu_l)}, \quad (11)$$

also that $\beta(\mu \rightarrow e\nu_e\nu_\mu) = 1$ and taking into account eq.(6) we can take the ratio between eq.(11) for $l = \tau, \mu$ to obtain:

$$\frac{\tau_\tau}{\tau_\mu} = \frac{\beta(\tau \rightarrow e\nu_e\nu_\tau)}{\beta(\mu \rightarrow e\nu_e\nu_\mu)} \left(\frac{m_\mu}{m_\tau} \right)^5 = (1.328 \pm 0.004) \times 10^{-7}. \quad (12)$$

This is consistent with the experimental lifetimes ratio $(1.3227 \pm 0.0005) \times 10^{-7}$. This agreement on lifetimes that differ on 7 orders of magnitude is a good proof that lepton universality holds on W decays at the tau mass scale.

Nonetheless, measurements from LHCb, BaBar and Belle experiments have shown consistent deviations from the SM predictions [6]. These experiments have independently measured a deviation on \bar{B} meson semi-leptonic branching ratios, especially:

$$R_D = \frac{\beta(\bar{B} \rightarrow D\tau^-\bar{\nu}_\tau)}{\beta(\bar{B} \rightarrow De^-\bar{\nu}_e)} \quad (13)$$

$$R_{D^*} = \frac{\beta(\bar{B} \rightarrow D^*\tau^-\bar{\nu}_\tau)}{\beta(\bar{B} \rightarrow D^*e^-\bar{\nu}_e)}. \quad (14)$$

The combined results for the different experiments are shown in Fig.3 . These measurements represent a 3.08σ deviation from the SM predictions, but even though they represent a hint of new physics, these results also have to be taken with care

since at this point it could be that systematic uncertainties are being underestimated or statistical deviations are larger than expected. In this matters, future analysis from experiments like LHCb and Belle with larger available datasets will be very important to untangle this situation.

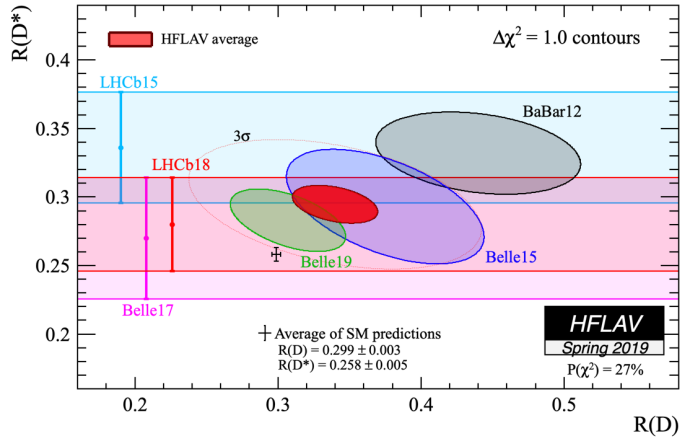


Figure 3: Combined results from BABAR,Belle and LHCb with $1-\sigma$ contour. The average calculated by the Heavy Flavour Averaging Group [2] is compared with the SM predictions.

3 Analysis

At the begining of this chapter, a review of the ATLAS detector at the LHC and a description of the reconstruction and identification of hadronic Tau decays on ATLAS are discussed. The last sections are devoted to describe the Analysis methodology of using $Z \rightarrow \tau\tau$ events to measure Monte Carlo correction factors for Tau identification algorithms on the high- p_T region.

3.1 The LHC and the ATLAS experiment

3.2 Tau Reconstruction and Identification on the ATLAS detector

Leptonically decaying taus (τ_{lep}), may have a higher impact parameter and tend to have a softer p_T spectrum compared with prompt W or Z boson decays to muons or electrons. These variables are not sufficient in principle to differentiate between τ_{lep} and prompt muons or electrons. In the case of hadronically decaying taus (τ_{had}), as we will see, there are a lot more variables we could use to tag the presence of a τ_{had} .

As we saw in section 2.1, τ_{had} decays can be classified in 1-prong or 3-prong, depending on the number of charged particles in the decay. A detailed review of the reconstruction procedure is discussed on [7]. τ_{had} candidates are seeded by jets using

the anti- k_t algorithm [8], with a distance parameter of 0.4. Jets are required to have $p_T > 10$ GeV and $|\eta| < 2.5$. Candidates between the barrel and forward calorimeter ($1.37 < |\eta| < 1.52$) are excluded due to poor instrumentation in this region.

The axis of the seed jet is defined by the energy-weighted barycentre of all clusters of calorimeter cells, called *TopoClusters* [9]. The τ_{had} vertex is defined as the vertex with the highest p_T -weighted fraction of all tracks with $p_T > 0.5$ GeV within a cone of $R = 0.2$ around the seed jet axis. Tracks within a cone of $R = 0.4$ are classified with a set of boosted decision trees (BDTs) into core and isolation tracks, the number of core tracks defines the number of prongs. Candidates with neither one or three tracks are rejected. Additionally, the sum of the charge of the tracks is required to be ± 1 .

The tau reconstruction algorithm does not provide discrimination against jets that could mimic the signal of a τ_{had} decay in the detector. Therefore, algorithms that perform this task have been developed. Previously, a BDT was used to discriminate jets against τ_{had} . Recently, a recurrent neural network (RNN) classifier that provides improved performance than the BDTs is in use [10].

The RNN makes use of a set of variables like: τ_{had} track features, information about energy deposits on the calorimeters clusters and high level features like the mass of the τ_{had} candidate tracks. These variables are used to exploit the differences in the shapes of the showers between τ_{had} and jets. In general, τ_{had} showers tend to be more collimated and to have fewer tracks than jets. A representation of this is shown in Fig.4.

Separated algorithms are trained for 1-prong and 3-prongs. The final RNN score assigned to each event corresponds to the fraction of rejected true τ_{had} , independent of p_T and number of interaction per bunch crossing (pileup). Four working points with increasing background rejection are defined to be used in physics analysis. The working points and background rejection factors are shown in Table 2. A plot

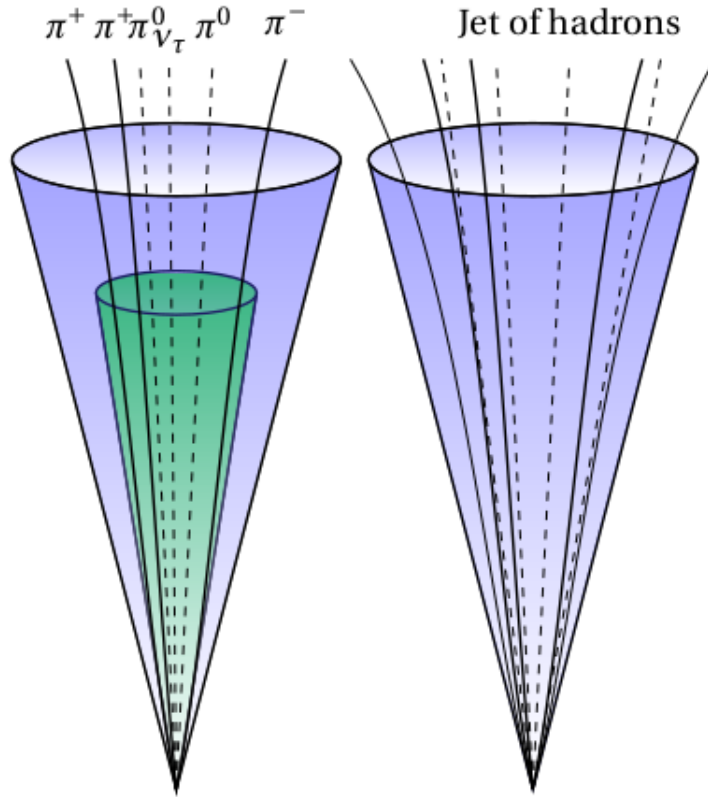


Figure 4: Graphic representation that shows the main differences between a 3-prong τ_{had} and a jet originated from quark or gluon radiation (QCD jets). Charged hadrons are shown as thick lines and dashed lines represent neutral particles. The green cone is drawn to depict how τ_{had} product decays are more collimated.

comparing the true τ_{had} selection efficiency versus the background rejection power for the RNN and BDT algorithm is shown in Fig. , the performance of the RNN is better than the BDT classifier. Finally, the distribution for the RNN score for true and fake τ_{had} is shown in Fig. , for both 1-prong and 3-prong decays.

Working point	Singal efficiency (%)		BG rejection BDT		BG rejection RNN	
	1-prong	3-prong	1-prong	3-prong	1-prong	3-prong
Tight	60	45	40	400	70	700
Medium	75	60	20	150	35	240
Loose	85	75	12	61	21	90
Very loose	95	95	5.3	11.2	9.9	16

Table 2: Working points with their corresponding true τ_{had} selection efficiency and the background rejection factors. The scores are shown for both RNN and BDT algorithms.

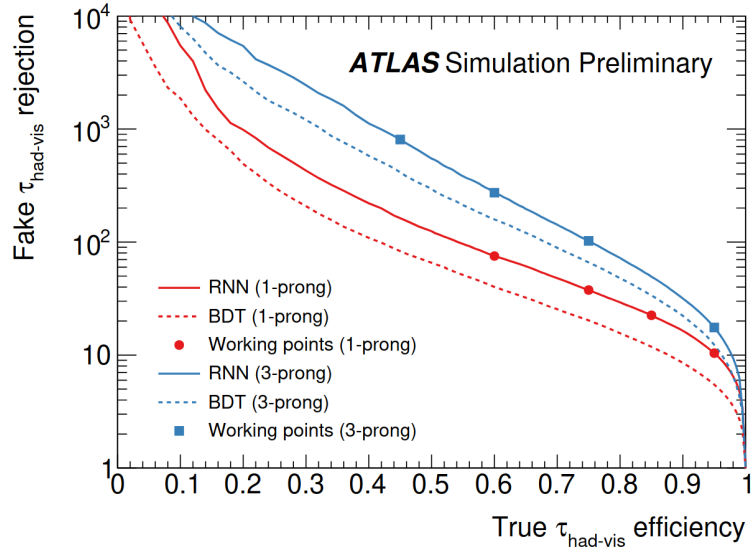


Figure 5: Comparisson between the performance of BDT and RNN algorithms. Working points are shown as points. Notice there is a trade off between true τ_{had} efficiency and background rejection power. Taken from [10]

3.3 Monte Carlo Samples

3.4 The Collinear Approximation

3.5 Event Selection

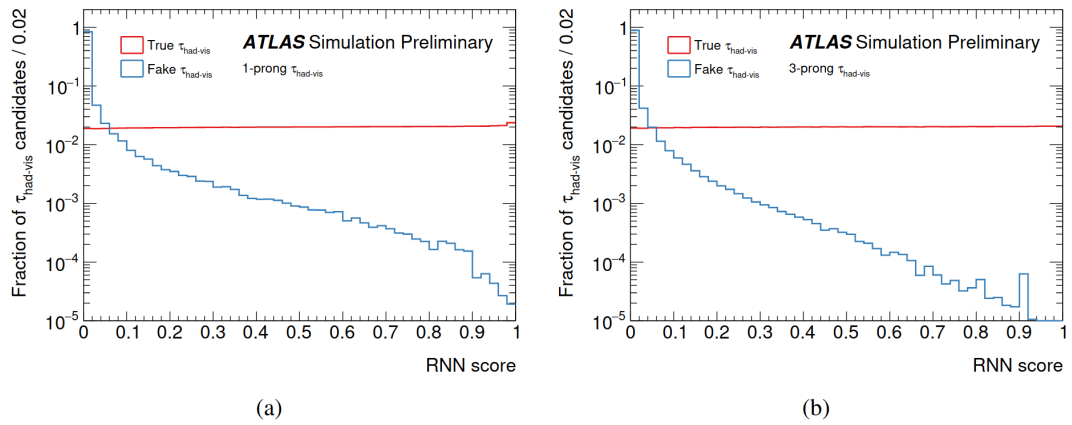


Figure 6: Distribution of the RNN scores for true and fake τ_{had} candidates for 1-prong (a) and 3-prong (b) cases. Taken from [10].

4 Results

The approach usually starts with the problem definition and continues with what you have done. Try to give an intuition first and describe everything with words and then be more formal like ‘Let g be ...’

4.1 $\mu\tau$ Final state

4.2 $e\tau$ Final state

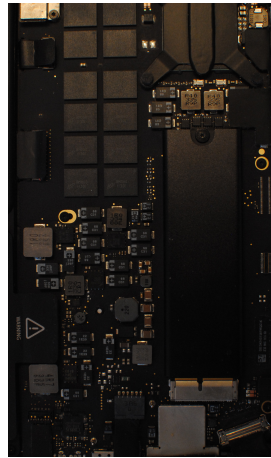
Start with a very short motivation why this is important. Then, as stated above, describe the problem with words before getting formal.

4.3 Monte Carlo and data discrepancies

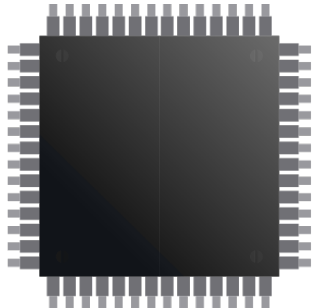
5 Conclusions and prospects

Type	Accuracy
A	82.47 ± 3.21
B	78.47 ± 2.43
C	84.30 ± 2.35
D	86.81 ± 3.01

Table 3: Table caption. foo bar...



(a) Some cool graphic



(b) Some cool related graphic

Figure 7: Caption that appears under the fig Lorem ipsum dolor sit amet, consectetuer adipiscing elit. Ut purus elit, vestibulum ut, placerat ac, adipiscing vitae, felis. Curabitur dictum gravida mauris. Nam arcu libero, nonummy eget, consectetuer id, vulputate a, magna. Donec vehicula augue eu neque. Pellentesque habitant morbi tristique senectus et netus et malesuada fames ac turpis egestas. Mauris ut leo. Cras viverra metus rhoncus sem. Nulla et lectus vestibulum urna fringilla ultrices. Phasellus eu tellus sit amet tortor gravida placerat. Integer sapien est, iaculis in, pretium quis, viverra ac, nunc. Praesent eget sem vel leo ultrices bibendum. Aenean faucibus. Morbi dolor nulla, malesuada eu, pulvinar at, mollis ac, nulla. Curabitur auctor semper nulla. Donec varius orci eget risus. Duis nibh mi, congue eu, accumsan eleifend, sagittis quis, diam. Duis eget orci sit amet orci dignissim rutrum.

Bibliography

- [1] M. Davier, A. Höcker, and Z. Zhang, “The physics of hadronic tau decays,” *Reviews of Modern Physics*, vol. 78, p. 1043–1109, Oct 2006.
- [2] H. F. A. Group, *Average of $R(D)$ and $R(D^*)$ for Spring 2019*, 2019.
- [3] M. L. Perl, G. S. Abrams, A. M. Boyarski, M. Breidenbach, D. D. Briggs, F. Bulos, W. Chinowsky, J. T. Dakin, G. J. Feldman, C. E. Friedberg, D. Fryberger, G. Goldhaber, G. Hanson, F. B. Heile, B. Jean-Marie, J. A. Kadyk, R. R. Larsen, A. M. Litke, D. Lüke, B. A. Lulu, V. Lüth, D. Lyon, C. C. Morehouse, J. M. Paterson, F. M. Pierre, T. P. Pun, P. A. Rapidis, B. Richter, B. Sadoulet, R. F. Schwitters, W. Tanenbaum, G. H. Trilling, F. Vannucci, J. S. Whitaker, F. C. Winkelmann, and J. E. Wiss, “Evidence for anomalous lepton production in $e^+ - e^-$ annihilation,” *Phys. Rev. Lett.*, vol. 35, pp. 1489–1492, Dec 1975.
- [4] M. Tanabashi, K. Hagiwara, K. Hikasa, K. Nakamura, Y. Sumino, F. Takahashi, J. Tanaka, K. Agashe, G. Aielli, C. Amsler, M. Antonelli, D. M. Asner, H. Baer, S. Banerjee, R. M. Barnett, T. Basaglia, C. W. Bauer, J. J. Beatty, V. I. Belousov, J. Beringer, S. Bethke, A. Bettini, H. Bichsel, O. Biebel, K. M. Black, E. Blucher, O. Buchmuller, V. Burkert, M. A. Bychkov, R. N. Cahn, M. Carena, A. Ceccucci, A. Cerri, D. Chakraborty, M.-C. Chen, R. S. Chivukula, G. Cowan, O. Dahl, G. D’Ambrosio, T. Damour, D. de Florian, A. de Gouvêa, T. DeGrand, P. de Jong, G. Dissertori, B. A. Dobrescu, M. D’Onofrio, M. Doser, M. Drees, H. K. Dreiner, D. A. Dwyer, P. Eerola, S. Eidelman, J. Ellis, J. Erler,

V. V. Ezhela, W. Fetscher, B. D. Fields, R. Firestone, B. Foster, A. Freitas, H. Gallagher, L. Garren, H.-J. Gerber, G. Gerbier, T. Gershon, Y. Gershtein, T. Gherghetta, A. A. Godizov, M. Goodman, C. Grab, A. V. Gritsan, C. Grojean, D. E. Groom, M. Grünewald, A. Gurtu, T. Gutsche, H. E. Haber, C. Hanhart, S. Hashimoto, Y. Hayato, K. G. Hayes, A. Hebecker, S. Heinemeyer, B. Heltsley, J. J. Hernández-Rey, J. Hisano, A. Höcker, J. Holder, A. Holtkamp, T. Hyodo, K. D. Irwin, K. F. Johnson, M. Kado, M. Karliner, U. F. Katz, S. R. Klein, E. Klempert, R. V. Kowalewski, F. Krauss, M. Kreps, B. Krusche, Y. V. Kuyanov, Y. Kwon, O. Lahav, J. Laiho, J. Lesgourgues, A. Liddle, Z. Ligeti, C.-J. Lin, C. Lippmann, T. M. Liss, L. Littenberg, K. S. Lugovsky, S. B. Lugovsky, A. Lusiani, Y. Makida, F. Maltoni, T. Mannel, A. V. Manohar, W. J. Marciano, A. D. Martin, A. Masoni, J. Matthews, U.-G. Meißner, D. Milstead, R. E. Mitchell, K. Mönig, P. Molaro, F. Moortgat, M. Moskovic, H. Murayama, M. Narain, P. Nason, S. Navas, M. Neubert, P. Nevski, Y. Nir, K. A. Olive, S. Pagan Griso, J. Parsons, C. Patrignani, J. A. Peacock, M. Pennington, S. T. Petcov, V. A. Petrov, E. Pianori, A. Piepke, A. Pomarol, A. Quadt, J. Rademacker, G. Raffelt, B. N. Ratcliff, P. Richardson, A. Ringwald, S. Roesler, S. Rolli, A. Romanouk, L. J. Rosenberg, J. L. Rosner, G. Rybka, R. A. Ryutin, C. T. Sachrajda, Y. Sakai, G. P. Salam, S. Sarkar, F. Sauli, O. Schneider, K. Scholberg, A. J. Schwartz, D. Scott, V. Sharma, S. R. Sharpe, T. Shutt, M. Silari, T. Sjöstrand, P. Skands, T. Skwarnicki, J. G. Smith, G. F. Smoot, S. Spanier, H. Spieler, C. Spiering, A. Stahl, S. L. Stone, T. Sumiyoshi, M. J. Syphers, K. Terashi, J. Terning, U. Thoma, R. S. Thorne, L. Tiator, M. Titov, N. P. Tkachenko, N. A. Törnqvist, D. R. Tovey, G. Valencia, R. Van de Water, N. Varelas, G. Venanzoni, L. Verde, M. G. Vincter, P. Vogel, A. Vogt, S. P. Wakely, W. Walkowiak, C. W. Walter, D. Wands, D. R. Ward, M. O. Wascko, G. Weiglein, D. H. Weinberg, E. J. Weinberg, M. White, L. R. Wiencke, S. Willocq, C. G. Wohl, J. Womersley, C. L. Woody, R. L. Workman, W.-M. Yao, G. P. Zeller, O. V. Zenin, R.-Y. Zhu, S.-L. Zhu, F. Zimmermann, P. A. Zyla, J. Anderson, L. Fuller, V. S. Lugovsky,

and P. Schaffner, “Review of particle physics,” *Phys. Rev. D*, vol. 98, p. 030001, Aug 2018.

- [5] E. Fermi, “Tentativo di una teoria dei raggi beta,” *Il Nuovo Cimento (1924-1942)*, vol. 11, no. 1, pp. 669–688, 1932.
- [6] G. Ciezarek, M. Franco Sevilla, B. Hamilton, R. Kowalewski, T. Kuhr, V. Lüth, and Y. Sato, “A challenge to lepton universality in b-meson decays,” *Nature*, vol. 546, p. 227–233, Jun 2017.
- [7] G. Aad *et al.*, “Identification and energy calibration of hadronically decaying tau leptons with the ATLAS experiment in pp collisions at $\sqrt{s}=8$ TeV,” *Eur. Phys. J. C*, vol. 75, no. 7, p. 303, 2015.
- [8] M. Cacciari, G. P. Salam, and G. Soyez, “The anti- k_t jet clustering algorithm,” *JHEP*, vol. 04, p. 063, 2008.
- [9] G. Aad *et al.*, “Topological cell clustering in the ATLAS calorimeters and its performance in LHC Run 1,” *Eur. Phys. J. C*, vol. 77, p. 490, 2017.
- [10] C. Deutsch, B. Martin dit Latour, and C. Grefe, “Identification of hadronic tau lepton decays using neural networks in the ATLAS experiment,” Tech. Rep. ATL-COM-PHYS-2019-773, CERN, Geneva, Jun 2018. RNN tau ID, ATL-PHYS-PUB-2019-033.

